Available online at www.sciencedirect.com
ScienceDirect
Journal of Volcanology and Geothermal Research 160 (2007) 42–58
Journal of volcanology and geothermal research
www.elsevier.com/locate/jvolgeores

The 1362 AD Öræfajökull eruption, Iceland: Petrology and geochemistry of large-volume homogeneous rhyolite

Rune S. Selbekk [a,b,c,*], Reidar G. Trønnes [a,c]

[a] Natural History Museum, Geology, University of Oslo, P.O. Box 1172 Blindern, N-0318 Oslo, Norway
[b] Mineralogisch-Geochemisches Institut, Albert Ludwigs University, Albertstr. 23b. D-79104 Freiburg, Germany
[c] Nordic Volcanological Center, Institute of Earth Sciences, Natural Sciences Building, IS-101 Reykjavik, Iceland

Received 14 March 2006; received in revised form 27 July 2006; accepted 8 August 2006
Available online 18 October 2006

Abstract

The ice-covered Öræfajökull stratovolcano is composed mostly of subglacial pillow lava and hyaloclastite tuff, ranging from basalt to rhyolite. A large devastating plinian eruption in 1362 AD produced 10 km^3 (2 km^3 DRE) rhyolitic ash and pumice from a vent within the summit caldera, with fallout mainly towards ESE. The ejected rhyolite magma with 0.5–1% crystals of oligoclase, fayalite, hedenbergite, ilmenite and magnetite was remarkably homogenous throughout the eruption.

A 1.8 m thick tephra section on the SE flank of the volcano has 14 recognizable units. The tephra is dominated by fine-grained vesicular glass with bubble wall thickness of 1–5 μm. The high and even vesiculation of the glass indicates fast magma ascent and explains the extreme mechanical fragmentation within the eruptive column. The grain-size distribution indicates time-variable intensity of the plinian eruption with three evenly spaced phases of maximum fragmentation. An initial vent-clearing explosion produced phreatomagmatic debris with up to 35% lithic fragments. The low abundance (<3%) of lithic fragments during the subsequent eruption indicates that the conduit and vent remained stable. The tephra fallout deposit is characterized by upwards increasing pumice dimensions and occasional bomb-like pumice blocks, indicating less mechanical fragmentation during contraction and lowering of the plinian column.

A conservative estimate of 20–40 km^3 for the total volume of the magma reservoir is based on the erupted volume of highly differentiated and homogeneous rhyolite. The 365-year period between 1362 and a minor benmoreitic eruption in 1727, and the absence of currently detectable magma reservoirs in the crust below Öræfajökull show that differentiated crustal magma chambers feeding large plinian eruptions can be established and disappear on a 100–500 year timescale.

Keywords: Öræfajökull; Iceland; plinian eruption; homogeneous rhyolite; fayalite; hedenbergite; fractional crystallization; magma chamber

1. Introduction

The ice-covered Öræfajökull stratovolcano rests unconformably on a glacially dissected and isostatically uplifted Tertiary basalt pile at the southern termination of the Eastern Volcanic Flank Zone in SE Iceland (Prestvik, 1985) (Fig. 1). The NE–SW-trending 120-km-long off-rift volcanic zone, about 50 km east of the Eastern Rift

* Corresponding author. Natural History Museum, Geology, University of Oslo, P.O. Box 1172 Blindern, N-0318 Oslo, Norway. Tel.: +47 22 85 16 44; fax: +47 22 85 18 00.
E-mail address: r.s.selbekk@nhm.uio.no (R.S. Selbekk).

0377-0273/$ - see front matter © 2006 Elsevier B.V. All rights reserved.
doi:10.1016/j.jvolgeores.2006.08.005

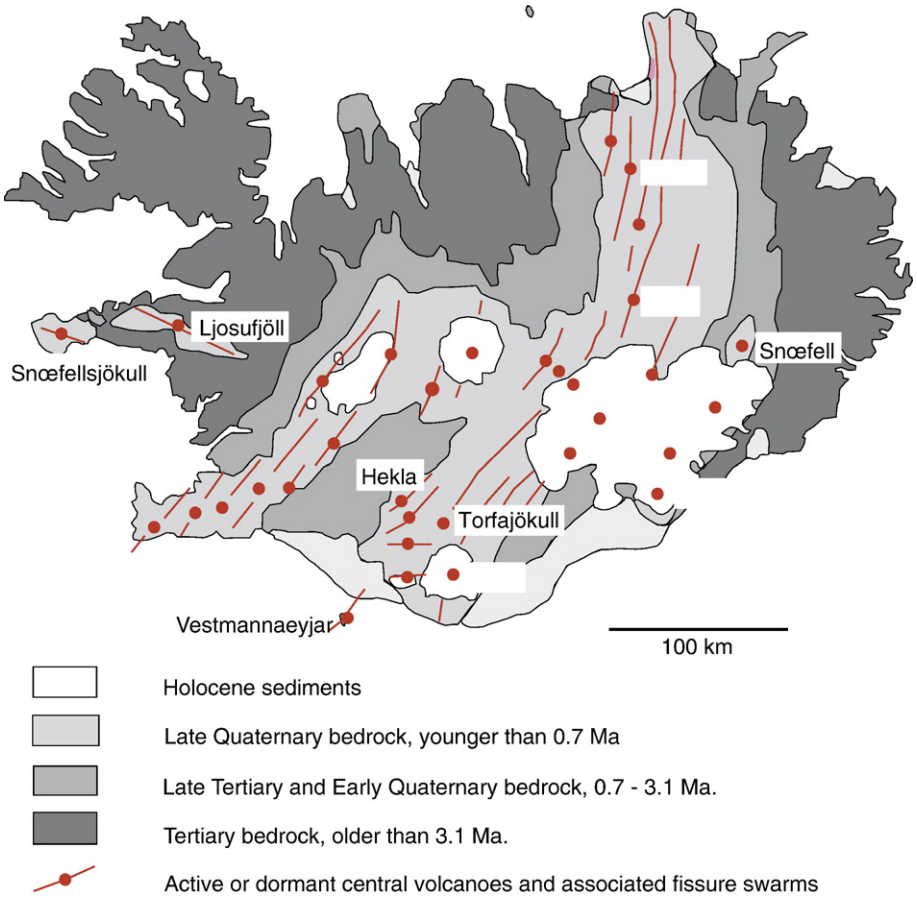

Fig. 1. Map of the Iceland, outlining the distribution of the major geological subdivisions. Modified after Johannesson and Saemundsson (1998).

Zone, is characterized by alkaline to tholeiitic transitional volcanism. The Öræfajökull edifice, reaching an altitude of 2119 m a.s.l., is dominated by subglacially erupted hyaloclastite units with pillow lava and tuff ranging from basalts to rhyolites (Prestvik, 1980, 1985).

The most recent Öræfajökull eruptions occurred in 1362 with a large plinian eruption and 1727 AD with a small benmoreitic eruption. The devastating 1362 eruptions was among the largest plinian eruption in historical time in Iceland. The eruption probably lasted for only 1 or 2 days and produced at least 10 km^3 rhyolitic tephra, corresponding to 2 km^3 dense rock equivalent (DRE) (Thorarinsson, 1958). The tephra fall was mainly to the east–southeast (Fig. 2), and the initial phase of the eruption was phreatomagmatic. The widespread deposit forms one of the volcanic marker horizons in sedimentary successions in the North Atlantic (Pilcher et al., 2005).

The present study of mineralogy, petrology, geochemistry and grain-size distribution of the rhyolitic tephra in a single section is based on the study of Thorarinsson (1958). The investigated profile is, to the authors' knowledge, the most extensive and complete section through the 1362 Öræfajökull tephra deposit.

We will try to partly reconstruct the magma chamber conditions and eruption dynamics of the 1362 event based on the mineralogy, petrology, geochemistry and grain-size distribution of the rhyolitic tephra. The large volume of remarkably homogeneous rhyolite erupted has important implications for the pre-eruption magma reservoir. The geochemical similarities with the Skærgaard and Bushveld granophyres will also be discussed.

2. General geology of the Öræfajökull volcanic system

The Late Tertiary volcanic basement southeast of Vatnajökull was deeply dissected by glacial erosion through a time span of 3 Ma (Helgason and Duncan, 2001). Parts of this isostatically uplifted volcanic sequence were formed by subglacial eruptions during the same interval (Prestvik, 1985). The currently active Öræfajökull volcano is built unconformably on this

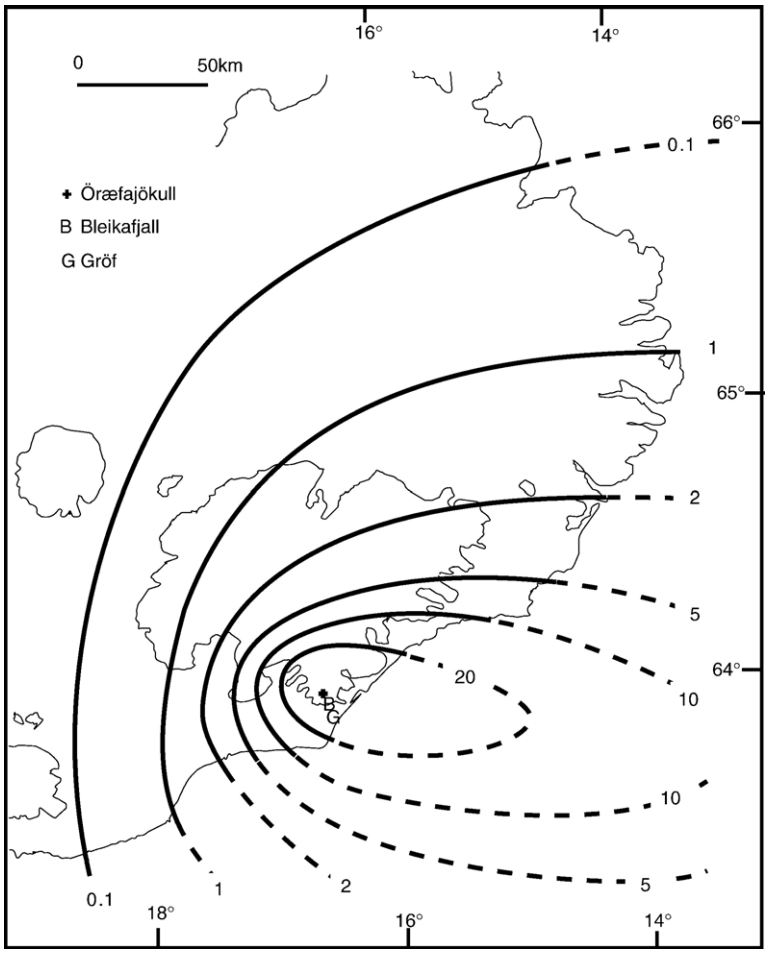

Fig. 2. Isopach map of the tephra units in cm for the 1362 eruption of Öræfajökull (modified from Thorarinsson, 1958).

elevated basement and forms the southwestern end of the NE-trending Eastern Volcanic Flank Zone (EVFZ). Most of the volcano is younger than 0.7 Ma (Brunhes, normally magnetized) but reversely magnetized rocks occur in lower parts of the edifice. The non-rifting EVFZ is parallel to, but 50 km southeast of the Eastern and Northern Rift Zones. The Icelandic volcanic flank zones have transitional alkalic to tholeiitic volcanism (Prestvik et al., 2001).

The crater rim surrounds an elliptical summit caldera with an area of 14 km^2 and unknown depth. The post-glacial activity in the summit area seems to have been almost exclusively explosive and tephrochronological studies in the neighborhood of the volcano show that this activity was rather limited and did not add much to the height and volume of the volcano (Thorarinsson, 1958).

The Öræfajökull stratovolcano is composed mostly of subglacially erupted pillow lava and hyaloclastite breccia and tuff covering a compositional range from basalt, via hawaiite, mugearite, benmoreite and trachyte to rhyolite (Prestvik, 1979, 1980, 1985; Prestvik et al., 2001). The rock suite is largely bimodal, with predominantly basaltic and rhyolitic compositions (Prestvik, 1980). Based on major element modeling Prestvik (1985) concluded that the intermediate lavas and some rhyolites were derived by fractional crystallization, but that most rhyolites were formed by partial melting of older crustal rocks. However, Prestvik et al. (2001) argued that the consistent O–Sr–Nd–Pb isotopic composition of the entire compositional spectrum from basalt to rhyolite is strong evidence that the intermediate and rhyolitic melts were produced by fractional crystallization of basaltic parental magmas.

3. The 1362 Öræfajökull eruption

Thorarinsson (1958) provides an extensive overview of the 1362 eruption, based on written accounts and studies of numerous tephra sections. The following short

review is based on Thorarinsson's account. The main eruption in June 1362 was purely explosive and rhyolitic, with the vent(s) located within the caldera. The regular and uniform tephra fall distribution (Fig. 2) indicates that the plinian phase was short-lived, probably 1–2 days.

The estimated total volume of the tephra layer from the 1362 eruption on land and sea is 10 km^3, corresponding to 2 km^3 DRE. The total area within the 0.1 cm isopach is estimated to nearly 300,000 km^2, and the tephra has been recognized in peat bogs in Scandinavia (Pilcher et al., 2005) and as a large particle pike in ice cores at Summit, Greenland (Palais et al., 1991).

The eruption caused several glacial lahars (jökulhlaups) on the west–southwest and to the southeast side of the volcano (Thorarinsson, 1958). These floods destroyed some farms, but most of the devastation was caused by tephra fall from the eruption (Thorarinsson, 1958). Before the eruption, the Öræfi district was one of the most productive agricultural areas in Iceland, and at least 30 farms were destroyed and abandoned for decades after the eruption. Rural settlements as far as 70 km east of Öræfajökull were damaged by the tephra fall, and many were abandoned for several years. Another explosive eruption of benmoreitic composition (T. Prestvik, personal

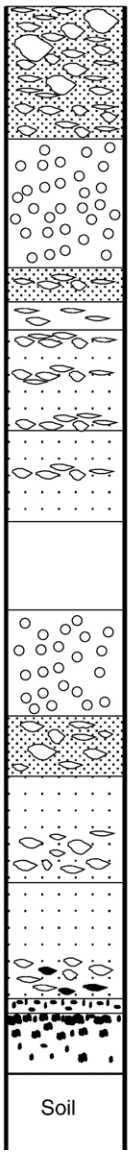

Layer 1. 24 cm. Inversely graded fine- to coarse-grained tephra, slightly eroded at top. Pumice fragments up to more than 60 cm.

Layer 2. 21 cm. Fine-grained tephra with centimeter-sized accretionary lapilli. Pumice fragments up to 3 cm

Layer 3. 6 cm. Corse to fine grained tephra. Pumice fragments up to 14 cm.

Layer 4. 5 cm. Fine-grained tephra, w/ pumice fragments up to 4.8 cm.

Layer 5. 17 cm. 3 layers reversely graded fine- to coarse- grained.

Layer 6. 15 cm. Reversely graded fine to coarse-grained tephra. Pumice fragments up to 5.2 cm together with some black lithic fragments.

Layer 7. 15 cm. Fine-grained tephra, but a little coarser than layer 8. Pumice fragments up to 4,4 cm.

Layer 8+9. 18 cm. Fine-grained tephra with centimeter-sized accretionary lapilli. The lower 10 cm (Layer 9) is more fine-grained than the upper part (Layer 8) but contains pumice fragments 5.8 cm.

Layer 10. 10 cm. Coarse-grained tephra w/ pumice fragments up to 7.5 cm

Layer 11. 18 cm. Reversely graded, fine- to coarse-grained tephra. Pumice fragments up to 3.6 cm.

Layer 12. Normally graded bed. Some lithic fragments together with the most pumice rich part of it. Pumice fragments up to 8.5 cm.

Layer 13. 3 cm. Fine-grained white to clear rhyolitic tephra. Lithic fragments form a 2-3 mm thick black upper most layer.

Layer 14. 10 cm Fine-grained brown tephra with about 35% lithic fragments. The upper part has large amounts of lithic fragments or a lithic zone. The lowermost 2-3 cm is fine-grained tephra with clay-sized fragments.

Fig. 3. Stratigraphy of the tephra deposit from the 1362 eruption at Öræfajökull, measured at Bleikafjall about 4 km east of the crater.

communication) occurred in late August 1727. Its volume was small compared with the 1362 eruption and probably did not exceed 0.2 km^3 of tephra (Thorarinsson, 1958).

4. Description of the tephra layer

Three separate tephra sections of the 1362 Öræfajökull eruption were observed and measured initially. The thickest and most complete section at Bleikafjall (Figs. 2 and 3) about 4 km SSE of the summit crater was selected for further detailed study. The sections show no signs of cross-stratification, bedforms, ripples or other indication of surge or pyroclastic flow, or erosional disturbances in relation to glacial or fluvial activity. This suggests that the layers were deposited continuously during a single eruption. The lack of signs of depositional breaks between the layers and the occurrence of accretionary lapilli, as well as irregular and angular pumice, all indicate that the deposits represent a fallout sequence.

The 181 cm thick section at Bleikafjall can be divided into 14 separate units based on grain-size distribution and abundance of pumice and lithic fragments (Fig. 3). The units range in thickness from 3 to 24 cm. The tephra varies from translucent to white and gray. A colour change to light brown, caused by the lithic fragments, is found in the lower units 13 and 14 (Fig. 4). The slight colour changes through the rest of the sequence can possibly be related to variable oxidation of the ash layer.

5. Analytical methods

The grain-size distribution of the 1362 tephra was determined by two methods. The coarse fraction was sieved by hand, measuring the intermediate diameter of each particle. The fraction < 1 mm was analyzed by laser diffraction on a Malvern Mastersizer 2000 with a Hydro 2000 MU. Each sample was measured 3 times for 15 s at a pump speed of 2500 RPM. The interval from 0.25 to 1.0 mm was analyzed by both methods in order to check and calibrate the results.

Major and trace elements were analyzed by X-ray fluorescence spectrometry (XRF) using glass beads and

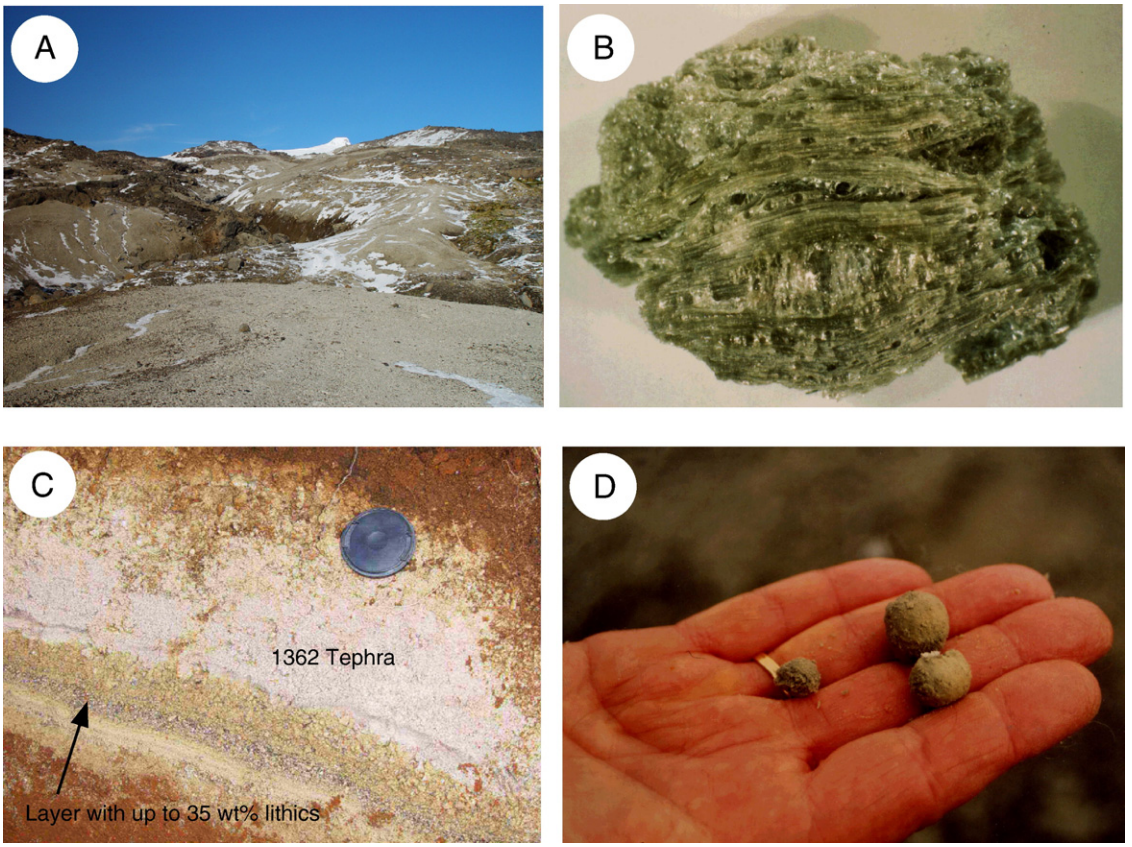

Fig. 4. (A) 1362 Tephra deposit at Bleikafjall, 4 km from the crater rim. (B) Typical vesicular glass pumice, with bubble wall thicknesses of 1–5 μm. (C) Tephra profile at Gröf showing the lithic-rich layer in the bottom of the 1362 eruption deposit. (D) Accretionary lapilli from the Bleikafjall deposit.

Table 1
Whole-rock analyses of tephra from the 1362 eruption at Öræfajükull

	Sample														1σ, 1–12
	1	2	3	4	5	6	7	8	9	10	11	12	13	14	
SiO_2	69.4	69.5	69.5	69.7	69.5	69.3	69.2	69.1	69.1	69.1	69.5	70.0	68.9	65.8	0.17
TiO_2	0.29	0.30	0.27	0.30	0.30	0.29	0.28	0.28	0.29	0.28	0.28	0.27	0.36	0.71	0.01
Al_2O_3	12.9	13.0	13.1	13.2	13.2	13.1	13.0	13.1	13.3	13.0	13.3	13.3	13.3	13.7	0.11
FeO_t	3.77	3.74	3.73	3.97	3.93	3.84	3.74	3.83	3.91	3.85	3.85	3.80	4.27	5.82	0.08
MnO	0.10	0.10	0.10	0.10	0.11	0.10	0.10	0.10	0.10	0.10	0.10	0.10	0.10	0.12	0.003
MgO	0.09	0.06	0.07	0.09	0.05	0.03	0.01	0.04	0.06	0.04	0.06	0.04	0.16	0.63	0.02
CaO	1.16	1.13	1.08	1.15	1.19	1.16	1.13	1.16	1.19	1.12	1.14	1.09	1.28	1.71	0.03
Na_2O	5.14	5.33	5.40	5.25	5.45	5.39	5.32	5.36	5.39	5.37	5.50	5.49	5.16	4.63	0.09
K_2O	3.16	3.28	3.32	3.28	3.25	3.29	3.32	3.29	3.25	3.30	3.29	3.34	3.24	2.90	0.04
P_2O_5	0.03	0.03	0.03	0.02	0.03	0.03	0.03	0.03	0.02	0.03	0.02	0.02	0.04	0.09	0.005
LOI	2.24	2.54	2.19	2.19	1.84	2.17	2.09	2.36	1.98	2.10	2.07	2.32	2.08	2.82	0.18
Sum	98.29	98.98	98.79	99.29	98.84	98.71	98.15	98.72	98.60	98.29	99.14	99.73	98.81	98.96	
Cl	1315	1352	1337	1346	1284	1370	1367	1326	1332	1358	1355	1416	1140	991	33
S	595	574	617	647	520	675	617	546	654	509	460	564	430	529	65
Rb	77	76	77	76	75	76	76	77	74	76	77	78	76	69	1
Sr	75	72	68	72	79	70	70	68	78	72	73	67	81	110	3
Ba	592	577	575	571	571	587	581	587	594	562	592	579	590	554	10
Y	110	110	110	109	110	110	110	110	109	110	109	109	110	101	1
Zr	755	756	757	764	782	766	769	761	768	767	765	762	755	697	7
V	5	8	4	5	4	3	6	3	6	4	6	–	13	61	2
Nb	76	76	76	75	76	75	76	77	74	75	76	76	75	72	1
Th	11	10	11	11	9	13	12	12	12	13	12	11	12	11	1
Sc	3	4	1	2	3	3	2	2	2	2	4	1	2	6	1
Zn	155	153	153	155	157	154	154	154	155	154	155	155	157	156	1
Ga	28	28	28	28	28	28	28	29	28	28	28	28	29	27	1

Major elements in wt.%, trace elements in ppm.

pressed powder pellets, respectively, at the Universities of Tromsø (1998, whole-rock tephra samples) and Freiburg (2006, whole-rock pumice fragments from selected samples). The estimated analytical precision is listed in Tables 1 and 2 (1σ). The total compositional ranges of the tephra samples (1–12), recording minor crystal fractionation in the eruption column (0.8–3.8 wt.% crystal content), correspond to about 4σ. The compositional variation of the pumice samples with 0.5–1 wt.% crystal content, however, corresponds to about 2σ. The minor deviations between the whole-rock tephra and pumice fragment compositions in absolute terms are caused by interlaboratory bias between the Tromsø and Freiburg XRF-laboratories.

Polished sections of pumice fragments from 6 selected samples were analyzed by wavelength-dispersive electron microprobe at the Institut für Mineralogie, Petrologie und Geochemie, Albert-Ludwigs-Universität Freiburg. Operating conditions were 15 kV, with a beam current of 8 nA. In order to minimize sodium loss, sodium was counted first for 8 s, then the other elements for 20 s. The analytical accuracy is considerably lower than that of the tephra XRD analyses, partly related to Na-migration under the electron beam. In spite of our efforts to reduce these effects, it seems clear that the analyses suffer from considerable Na-deficiency. Based on the analysis of glass standards, we estimate this deficiency to be 10–20%.

Mineral grains and lithic fragments were separated from the glass by panning under water, followed by heavy liquid separation and handpicking. The mineral separates were mounted in epoxy and polished, prior to mineral analysis by wavelength-dispersive electron microprobe at the Nordic Volcanological Institute, University of Iceland (rebuilt and upgraded 7-channel ARL-SEMQ instrument). The detectors for Si, Al, Fe and Ca have fixed positions and the three remaining detectors are mobile, motor-driven spectrometers. Natural and synthetic standards were used for calibration, and the data were corrected for background using a mean atomic number procedure. Operating conditions were 20 nA and 15 kV, except for feldspar, which was analyzed with a beam current of 10 nA in order to minimize sodium loss. Based on repeated analyses of standards and samples, the analytical error (1σ) appears to exceed the extremely limited compositional variations of each of the minerals plagioclase, clinopyroxene and olivine (Table 3).

Table 2
Composition of whole-rock pumice fragments in selected tephra layers from the Öræfajökull, 1362 eruption

	Sample						1σ
	1	3	5	8	9	12	
SiO_2	70.3	70.4	70.0	70.0	70.3	69.9	0.19
TiO_2	0.25	0.26	0.26	0.26	0.26	0.26	0.00
Al_2O_3	13.1	13.1	13.1	13.2	13.0	13.1	0.07
FeO_t	3.37	3.38	3.35	3.32	3.38	3.41	0.03
MnO	0.10	0.10	0.10	0.10	0.10	0.10	0.00
MgO	0.02	0.02	0.02	0.03	0.01	0.02	0.01
CaO	1.06	1.07	1.08	1.12	1.06	1.10	0.02
Na_2O	5.55	5.57	5.60	5.64	5.57	5.55	0.03
K_2O	3.28	3.31	3.28	3.23	3.30	3.25	0.03
P_2O_5	0.02	0.02	0.02	0.02	0.02	0.02	0.00
LOI	1.46	1.49	1.51	1.58	1.39	1.78	0.14
Sc	2	3	2	2	3	1	0.8
V	6	6	7	7	6	6	0.5
Co	2	2	3	3	2	3	0.6
Ni	3	4	4	4	4	4	0.4
Cu	5	5	6	4	6	3	1.2
Zn	152	150	149	146	151	149	2.1
Ga	30	31	31	31	31	30	0.5
Rb	73	77	77	73	76	74	1.9
Sr	61	62	67	72	61	67	4.4
Y	114	119	120	114	120	112	3.6
Zr	737	756	741	737	757	745	9.0
Nb	79	82	82	80	83	78	2.0
Ba	624	621	613	624	623	621	4.2
Hf	17	16	16	16	16	16	0.4
Ta	3	9	5	8	4	10	2.9
Pb	9	8	10	9	9	10	0.8
Th	12	12	10	11	10	11	0.9
U	3	2	5	4	5	4	1.2

Major elements in wt.%, trace elements in ppm. XRF analyses carried out at Geochemisches Institut, Albert Ludwigs University.

Table 3
Mineral compositions of the 1362 Öræfajökull tephra from units 1 to 14

	Mineral		
	Pl (1σ)	CPX (1σ)	Ol (1σ)
SiO_2 (wt.%)	64.6 (1.0)	47.7 (1.0)	29.8 (0.6)
TiO_2 (wt.%)	–	0.48 (0.11)	–
Al_2O_3 (wt.%)	21.3 (0.4)	0.37 (0.09)	–
FeO_t (wt.%)	–	29.5 (0.6)	65.7 (1.0)
MnO (wt.%)	–	1.09 (0.16)	2.79 (0.20)
MgO (wt.%)	–	0.80 (0.16)	0.11 (0.03)
CaO (wt.%)	2.92 (0.20)	19.5 (0.6)	0.51 (0.12)
Na_2O (wt.%)	9.43 (0.47)	0.07	–
K_2O (wt.%)	0.94 (0.14)	–	–
Cr_2O_3 (wt.%)	–	0.02	–
Sum	99.15	99.48	98.88

The analyses cover 1–4 analytical spots on 8–15 grains of each mineral in each of the 14 tephra units.
Pl = $An_{14}Ab_{81}Or_5$ oligoclase.
Average of 150 EMP analyses.
CPX = $Wo_{44.7}En_{2.6}Fs_{52.7}$ hedenbergite.
Average of 140 EMP analyses.
Ol = $Fa_{99.7}Fo_{0.3}$ fayalite.
Average of 135 EMP analyses.
(–) Below detection.

6. Grain-size distribution and proportion of crystals and lithic fragments

The fallout is extremely fine-grained vesicular glass with bubble wall thicknesses of 1–5 μm. Needle-like glass fragments in the pumice indicate exsolution of magmatic gases and vesiculation of the melt during fast magma ascent. The grain-size fraction less than 0.25 mm makes up 53–84 wt.% of the samples, and the grain-size spectra have 3 distinct peaks with maximum fragmentation (Figs. 5 and 6).

The total amount of phenocrysts in the pumice samples is 0.5 to 1 wt.%, based on the measured proportions in larger pumice fragments in this section. This is considered to be representative of the crystal content of the magma. The mineral proportion in the bulk fallout tephra is between 0.5 and 3.8 wt.% and negatively correlated with the proportion of the finest grain size fractions of the tephra. The variation in mineral content between pumice and tephra is related to gravitational separation in the fallout column. Oligoclase, fayalite and hedenbergite constitute 50–80, 10–25, and 10–25 wt.% of the phenocryst populations, respectively.

The grain-size distribution shows that the eruption proceeded in three successive stages. Whereas the initial phreatomagmatic stage produced debris with 12–35% lithic fragments in the grain-size fraction 1–0.25 mm (samples 13 and 14), the lithic fragment content is below 3% in the rest of the section. The lithic fragment population is dominated by basalt and rhyolite, but minor amounts of hyaloclastite tuff, andesitic and trachytic lavas, chalcedony, and shale are also present. In distal facies of the fallout tephra, the initial phase is recognized as a pale brownish basal layer with about 3% lithic fragments below the otherwise white glassy ash (Thorarinsson, 1958).

7. Geochemistry

7.1. Tephra composition

The major and trace element analyses for the bulk tephra samples show remarkably similar compositions,

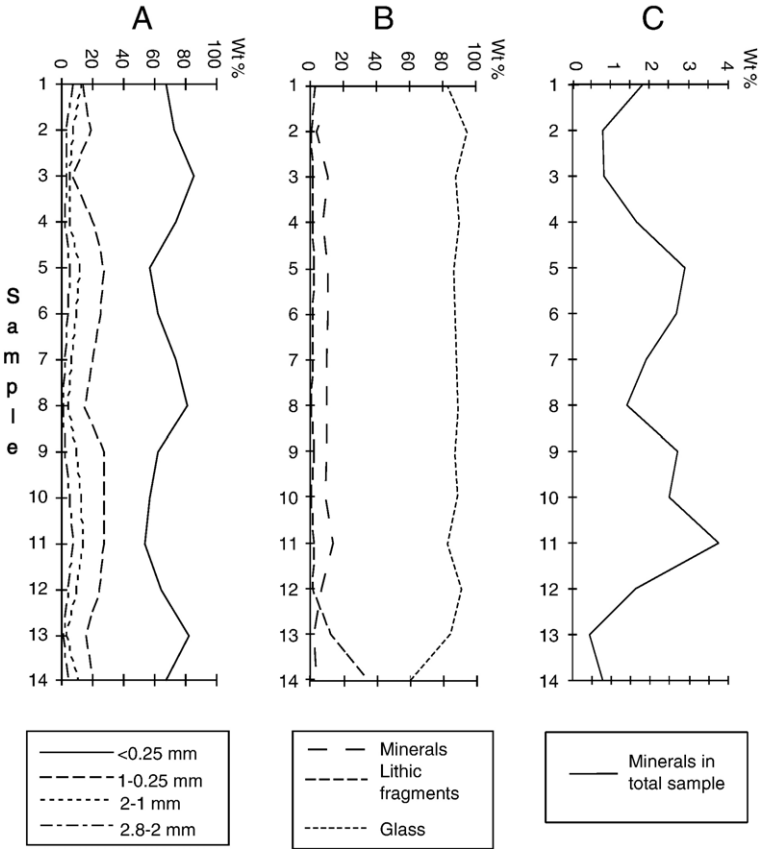

Fig. 5. (A) Grain-size distribution of tephra from the 1362 eruption of Öræfajökull. (B) Distribution of lithic fragments, glass and minerals in the grain-size fraction between 1.0 and 0.25 mm. The large amount of lithic fragments in samples 13 and 14 (<30 wt.%) and low amounts in the rest of the samples (>5 wt.%) show that the eruption was a continuous eruption from a single vent. (C) Distribution of minerals in total sample.

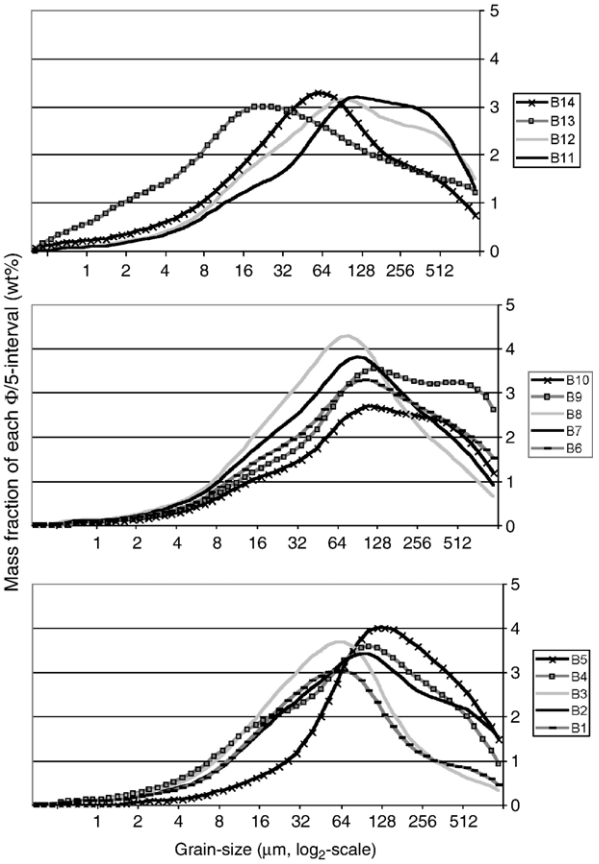

Fig. 6. Grain-size distribution of grains smaller than 2 mm, showing the variation in fragmentation and intensity during eruption.

except for the stratigraphically lowest samples, 13 and 14 (Table 1). The compositions of samples 13 and 14 are related to high contents of lithic fragments, and the bulk tephra chemistry of these samples will not be considered in the following discussion. The total range of major and trace element abundances of samples 1–12 is very limited and comparable to the estimated 4σ-range of the XRF analyses (Table 1, Fig. 7). Weak, but significant, correlations between various elements and the total mineral content recorded for each sample are consistent with the observed phenocryst assemblage of oligoclase, fayalite and hedenbergite in proportions 4:1:1 (weight proportions). Most of the major elements and some of the trace elements are shown as functions of the total crystal content of the tephra in Fig. 7. The elements enriched in the minerals relative to the melt (e.g. Al, Na, Ca, Fe, Ti, Mn, Sr, and Ba) are positively correlated with the crystal content, whereas other elements (e.g. Si, K, Rb, Cl, S and H, expressed as LOI (loss on ignition)) show weak negative correlations with the mineral content. This observation indicates that the glass composition throughout this tephra section is even more homogeneous than the whole-rock tephra samples with total crystal contents of 0.8–3.8% (i.e. samples 1–12).

Our best estimate for the glass compositions are derived from the intersection of least squares regression lines (element concentration as function of the total crystal content) with the zero percent mineral axes. Because the analytical uncertainty is considerably lower for the XRF analyses than for the EMP analyses, this estimate is probably a more reliable value for the melt composition than the direct melt analyses. The relative changes between the linear regression values for 0% and 3.75% crystals are greatest for the volatile content, expressed by the LOI value. LOI is 23% higher in the 100% melt composition, indicating that fractional crystallization enriches the melt in H and S. Water is clearly the dominant volatile component, because the total variation in S and Cl is only 150–200 ppm and minor variations in the oxidation state of Fe cannot affect the LOI variation to a significant extent. The relatively large increase in water content expressed as LOI from the tephra with more than 2.5% crystals to tephra with less than 1% crystals may, however, largely be related to the accompanying glass fragmentation increase and attributed to depositional processes in the fallout from the eruption column.

The composition of the 1362 AD rhyolite is similar to other rhyolites from Öræfajökull (Prestvik, 1985). The Al_2O_3 (13.1 wt.%) and K_2O (3.28%) contents are lower and higher, respectively, compared to Icelandic rift zone rhyolites at a corresponding SiO_2 content of 69.4% (e.g. Oskarsson et al., 1982; Nicholson et al., 1991). Furthermore, the contents of P_2O_5 (0.03%) and Na_2O (5.37%) are higher, and that of CaO (1.14%) is lower, than in corresponding rift zone rhyolites (0.01%, 3.9% and 2.7%, respectively, at the 69.4% SiO_2 level for the Krafla compositional trends of Nicholson et al., 1991).

7.2. Pumice composition

Additional whole-rock analyses of pumice fragments from six selected tephra layers were performed in order to further investigate the potential effects of gravitational fractionation of crystals and glass in the eruption column (Table 2). The compositional variation of the pumice, corresponding to about 2σ (Table 2), is slightly smaller than the compositional range of the tephra samples 1–12. The minor interlaboratory deviations between the Tromsø and Freiburg XRF-laboratories are larger than any detectable systematic variation between the pumice samples with a crystal content of 0.5–1 wt.% and the tephra samples (1–12) with 0.8–3.8 wt.%

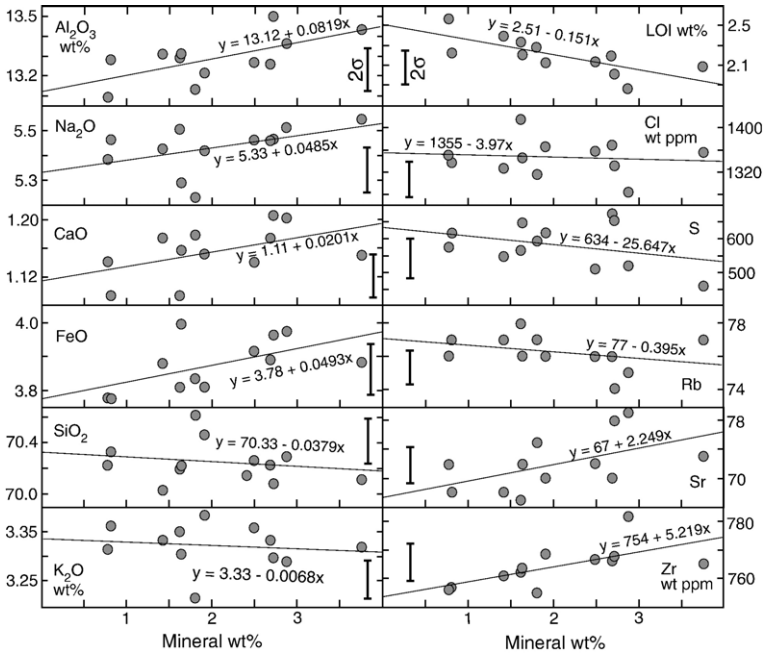

Fig. 7. Total mineral content (wt.%) versus major and trace elements in tephra samples 1–12. The analyses are normalized to 100% (including loss on ignition, LOI), and the thin lines are linear regression curves with associated equations. Estimated average 2σ error bars are shown for each of the elements or oxides. The linear regression equations are used to derive an estimate of the crystal-free melt composition (Table 5 and text).

crystals. The pumice composition therefore confirms the extremely homogeneous nature of the magma.

7.3. Glass composition

The glass samples have identical compositions within the estimated analytical uncertainty and they are compositionally similar to the whole-rock tephra (Table 4). However, the minor crystal content of the tephra results in slightly higher Si and K and lower Ti, Al, Fe, Ca and Na of the glass (Table 1). Due to the estimated Na-deficiency of 10–20% in our analyses, we compare the data assuming a 15% Na-deficiency. The pumice glass from the sampled tephra section and the linear regression estimate of melt compositions from the tephra analyses are compositionally identical within analytical uncertainty to glass shards from tephra horizons from the 1362 AD eruption sampled in the Öræfa district, Svinafell (10 km west of the summit), Lofoten (northern Norway) and northern Ireland (Sigurdsson, 1982; Palais and Sigurdsson, 1989; Pilcher et al., 1995; Larsen et al., 1999; Pilcher, 2005). A comparison of these analyses on a volatile-free basis (normalized to 100%) is presented in Table 5. The lack of variation exceeding the EMP-analytical uncertainty indicates that almost the entire erupted magma volume had a uniform composition. The analyses of assumed Öræfakull 1362 tephra in ice cores from the central Greenland ice cap (Palais et al., 1991), however, differ markedly from the compositions presented in Table 5. The unusually high silica content of 76.9 wt.% and the large analytical uncertainty quoted for these analyses indicate that this discrepancy may be due to analytical errors.

Table 5 also demonstrates that the average glass composition has slightly higher Si and K and lower Al, Na, Ca, Fe, Ti, Mn and Mg than the average tephra composition. Least squares mass balance fractionation

Table 4
Electron microprobe analysis of pumice glasses from the 1362 eruption at Öræfajükull

	Sample						Average	1σ
	1	3	6	9	13	14		
SiO_2	71.4	70.8	71.0	71.0	71.2	70.8	71.0	0.21
TiO_2	0.23	0.25	0.24	0.22	0.23	0.25	0.24	0.01
Al_2O_3	13.4	13.8	13.5	13.6	13.4	13.3	13.5	0.16
FeO_t	3.29	3.49	3.38	3.45	3.39	3.39	3.40	0.06
MnO	0.11	0.09	0.13	0.11	0.10	0.10	0.10	0.01
MgO	0.01	0.02	0.01	0.01	0.02	0.02	0.01	0.00
CaO	0.99	1.10	1.13	1.18	1.05	0.97	1.07	0.07
Na_2O	4.71	4.70	4.50	4.71	4.41	4.22	4.54	0.18
K_2O	3.40	3.31	3.34	3.37	3.39	3.41	3.37	0.03
Sum	97.75	97.74	97.41	97.92	97.43	96.67	97.49	0.41

Major elements in wt.%.

Table 5
Comparison of analyses of tephra and glass from the Öræfajökull, 1362 eruption

	SiO_2	TiO_2	Al_2O_3	FeO_t	MnO	MgO	CaO	Na_2O	K_2O
Tephra compositions									
Average composition, samples 1–12	71.9	0.30	13.6	3.97	0.10	0.06	1.18	5.55	3.40
Sample Ö162, Prestvik (1985)	71.2	0.28	13.9	3.65	0.11	0.00	1.29	6.10	3.51
Sample Ø1326, Thorarinsson (1958)	70.5	0.30	14.9	3.88	0.10	0.05	1.59	5.16	3.50
Sample Ø1326, Thorarinsson (1958)	71.6	0.33	13.6	3.66	0.11	0.02	1.29	5.95	3.45
Average tephra composition	71.3	0.30	14.0	3.79	0.11	0.03	1.34	5.69	3.46
1 standard deviation	0.58	0.02	0.61	0.16	0.01	0.03	0.18	0.42	0.05
Glass compositions									
Linear regression, 0% min. (samples 1–12)	72.2	0.29	13.5	3.87	0.10	0.07	1.14	5.47	3.42
Average glass analysis, samples 1, 3, 6, 9, 13, 14	72.5	0.24	13.8	3.47	0.11	0.02	1.09	5.33	3.44
Average glass, Sigurdsson (1982)	72.9	0.22	13.4	3.22	0.05	0.00	1.01	5.56	3.60
Matrix glass, Palais and Sigurdsson (1989)	73.3	0.27	12.9	3.12	0.02	0.01	1.01	5.73	3.62
Inclusion glass, Palais and Sigurdsson (1989)	72.7	0.16	13.1	3.45	0.10	0.00	0.94	5.82	3.65
Average glass, Svinafell, Larsen et al. (1999)	72.8	0.22	13.5	3.22	0.11	0.04	1.03	5.68	3.43
Average glass, Lofoten, Pilcher et al. (2005)	73.2	0.25	13.5	3.25	0.11	0.01	1.04	5.28	3.38
Average glass, Sluggan Bog, Pilcher et al. (1995)	72.9	0.30	13.7	3.35	0.00	0.03	1.03	5.24	3.48
Average glass	72.8	0.25	13.4	3.37	0.08	0.02	1.04	5.51	3.50
1 standard deviation	0.36	0.04	0.27	0.24	0.05	0.02	0.06	0.22	0.10
Measured and inferred pumice (with 0.8 wt.% minerals) composition									
Average pumice analysis (1, 3, 5, 8, 9, 12)	72.4	0.27	13.3	3.42	0.10	0.02	1.10	5.67	3.33
Linear regression of tephra at 0.8 wt.% min.	72.0	0.29	13.5	3.91	0.10	0.06	1.16	5.50	3.41

Linear regression estimate of glass composition (at 0% minerals) from tephra analyses of samples 1–12 (see Fig. 4). Wt.%: 70.3 SiO_2, 2.87 TiO_2, 13.1 Al_2O_3, 3.78 FeO_t, 0.10 MnO, 0.06 MgO, 1.11 CaO, 5.33 Na_2O, 3.33 K_2O, 0.03 P_2O_5, 2.51 LOI. Wt. ppm: 1355 Cl, 634 S, 77 Rb, 67 Sr, 575 Ba, 110 Y, 754 Zr, 5 V, 76 Nb, 11 Th, 1.5 Sc, 153 Zn, 28 Ga.
The compositions in the main table are normalized to 100%, and the Na_2O of the average glass composition for samples 1, 3, 6, 9, 13 and 14 is increased by 15% to compensate for observed Na-migration under the electron beam.

modeling relating the compositions and proportions of the minerals to various bulk tephra and glass compositions gives solutions that are consistent with the observed proportions of oligoclase, fayalite and hedenbergite (with or without minute quantities of ilmenite). However, the solutions generally overestimate the total mineral content of the tephra (3–9%), relative to the observed maximum mineral content of 3.8% in sample 11.

7.4. Mineral morphology and chemistry

The mineral assemblage of the 1362 tephra is composed primarily of euhedral to subhedral oligoclase and euhedral fayalite and hedenbergite. There is no sign of crystal resorption by the melt, and the crystal diameters are generally less than 1 mm for plagioclase and about 0.5 mm for olivine and clinopyroxene. Ilmenite and titanomagnetite occur as inclusions in clinopyroxene and olivine. The small and mostly euhedral silicate phenocrysts are remarkably homogenous with no detectable zonation, indicating that the minerals are in or close to compositional equilibrium with the erupted rhyolite melt. The entire compositional variation is within the analytical precision (Table 3).

The mineral compositions are shown in Fig. 8. The oligoclase crystals have composition $An_{14}Ab_{81}Or_{5.5}$. The hedenbergites occur as long prismatic crystals, and contain inclusions of ilmenite, titanomagnetite and glass. The hedenbergite composition is $Wo_{44.7}En_{2.6}Fs_{52.7}$. The fayalite phenocrysts ($Fa_{99.7}Fo_{0.3}$) contain inclusions of ilmenite, titanomagnetite, pyroxene and glass. Some of the fayalite crystals show indications of rapid crystallization with elongated glass inclusions parallel to the *c*-axis.

The included oxides have occasionally characteristic octahedral shapes. Black metallic hexagonal plate-shaped crystals of hematite are observed in all layers, except layers 13 and 14, indicating oxidation of the melt during the eruption.

8. Discussion

The investigated tephra section, located 7–8 km from the main crater, documents the uniform mineralogy and chemistry of the erupted magma and the overall intensity of the main plinian eruption. Although this section cannot provide complete information about the entire magma volume, additional analyses of glass shards from the

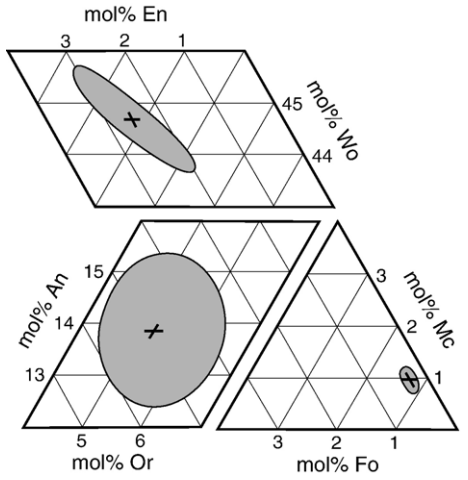

Fig. 8. Mineral compositions (Table 3) recalculated and displayed in triangular diagrams An–Ab–Or, Wo–En–Fs and Mc–Fo–Fa. The crosses and gray ellipses show the average value and the extent of 2σ variation of 150, 140 and 135 EMP analyses of plagioclase, pyroxene and olivine, respectively. The analytical error exceeds the extremely limited compositional variation of the minerals. Abbreviations: An, anorthite; Ab, albite; Or, orthoclase; Wo, wollastonite; En, enstatite; Fs, ferrosillite; Mc, monticellite; Fo, forsterite; Fa, fayalite.

associated tephra horizon covering a 3000 km wide area including Iceland, central Greenland, northern Norway and Ireland indicate that the entire erupted magma was uniform rhyolite with a melt compositional range comparable to or lower than the analytical uncertainty of the EMP analyses used. The whole-rock tephra analyses presented by Thorarinsson (1958) and Prestvik (1985) are probably also identical to our analyses within analytical errors.

The field relations, including accretionary lapilli and angular pumice fragments, demonstrate that the investigated sections of 1362 AD Öræfajökull tephra represent in-situ airfall deposits. The high proportion of lithics in the lowermost tephra unit indicates that the eruption started with a major conduit- and vent-opening explosion event, followed by a relatively constant jet through an open conduit. The lithic fragment content is a sensitive indicator of the competence and stability of the conduit wall rocks. The undisturbed nature of the airfall tephra sections at relatively high-altitude locations near the summit crater of Öræfajökull indicates that the volcano did not have a very thick ice cover before the eruption. Historical accounts, confirm a thin summit glacier prior to the eruption (e.g. Thorarinsson, 1958). Accretionary lapilli found in the fine-grained tephra layers are generally assumed to be diagnostic of combined ashfall and rain. High air humidity may also be related to a steam-rich eruption column caused by melting of the ice cover.

The negative correlation between fragmentation level and crystal content may be related to differential settling velocity in the fallout zone to the eruption column. During periods of high wind speed and/or turbulence the coarser ash and pumice fragments as well as the denser mineral fragments will settle preferentially nearer the source than the finer ash. These stratigraphic variations in grain size may reflect intensity variations in the eruption column.

8.1. Magma chemistry, equilibrium conditions and volatile content

The extreme compositional homogeneity of the glass and phenocrysts of the 1362 AD tephra is remarkable for a rhyolitic eruption unit of 2 km^3 DRE. The homogeneity of melt and minerals and the uniform and low crystal content of the tephra throughout the eruption indicate a well-equilibrated magma reservoir. It is possible that the erupted tephra was extracted only from the upper portions of a much larger and compositionally zoned reservoir.

There are almost no other documented examples of rhyolites or granites with crystallization assemblages very similar to the Öræfajökull 1362 AD tephra. Whereas other rhyolites from the Öræfajökull complex have similar bulk composition and phenocryst mineralogy (Prestvik, 1985), they do not have plagioclase, olivine and clinopyroxene with as high proportions of the albite, fayalite and hedenbergite end members as the 1362 AD tephra.

The other examples of crystallization assemblages that most closely match the 1362 tephra seem to be the granophyres of the late-stage differentiates of the Skaergaard and Bushveld complexes (e.g. Wager and Brown, 1968). The most differentiated cumulus mineral assemblages observed in both Skaergaard and Bushveld are An_{30}, Fo_0 and $Wo_{42–43}En_{0–1}Fs_{57}$. Both of these assemblages include magnetite and the Skaergaard assemblage also includes ilmenite and apatite. The similarity with the 1362 tephra is close, although the 1362-tephra plagioclase is considerably more albitic than the granophyre plagioclase. The assumed parental magma compositions of the Skaergaard intrusion and the Öræfajökull volcanic system (e.g. Prestvik, 1985; Nielsen, 2004, Trønnes et al., unpublished analyses) are similar high Fe–Ti–tholeiitic basalts. The higher (Na+K)/Ca and (Na+K)/Al ratios in the Öræfajökull tholeiites (0.39 and 0.27, respectively) compared to the Skaergaard parental magma estimate (0.29 and 0.21, respectively) may explain the higher proportions of albite and orthoclase in the most differentiated plagioclase of the Öræfajökull tephra. The Skaergaard granophyre compositions are also broadly similar to

the 1362 tephra, but with considerably lower (Na+K)/Ca and (Na+K)/Al ratios (Wager and Brown, 1968).

The almost pure fayalite and hedenbergite mineral compositions of the 1362 magma make it difficult to model the P–T conditions of the mineral–melt equilibria with common thermodynamics-based software. The mineral–melt assemblage does indicate, however, that the water and oxygen fugacities of the magma were relatively low. The simultaneous incipient crystallization of oligoclase ($Ab_{81}Or_5$), fayalite, hedenbergite and Fe–Ti-oxides reflects a melt composition with high Fe, Ti, Na and K, relative to Mg, Ca and Al.

The lack of hydrothermal activity in the Öræfajökull area may indicate that the magma evolution and differentiation occurred in deep crustal reservoirs. The crust under Vatnajökull is 30–40 km thick (Kaban et al., 2002) and a deep-seated magma chamber system is possible. Multiple magma reservoirs have been inferred elsewhere in Iceland, e.g. in relation to the 1984 Krafla eruption (Tryggvason, 1986). Hildreth (1981) suggested that large eruptions of non-basaltic magma tap thermally and compositionally zoned magma reservoirs. Normally, as the eruptions proceed, successively deeper magma chamber levels may be tapped, until eventually more mafic scoria accumulates on top of the earlier erupted silicic pumice. Many of the largest plinian eruptions from Icelandic volcanoes have resulted in tephra deposits grading upwards from silicic pumice to intermediate and basaltic scoria. In particular, the large Holocene eruptions from the Hekla volcano (H5–, H4–, H3– and 1104 AD), each delivering on the order of 1 km^3 DRE, have these characteristics (Thorarinsson, 1967). The homogenous 1362 AD Öræfajökull tephra may conceivably represent the uppermost portions of a zoned magma reservoir system considerably larger than the Hekla reservoirs. Katla, another of the Icelandic flank zone volcanoes, appears to have separate but contemporaneously active basaltic and rhyolitic magma reservoirs located under the central and peripheral parts of the 9–14 km wide caldera, respectively (Larsen et al., 2001; Soosalu and Einarsson, 2004).

Beard and Lofgren (1989, 1991) determined the compositional characteristics of silicic melts in equilibrium with metabasaltic lithologies at 0.1–0.3 GPa at H_2O-saturated and H_2O-undersaturated (dehydration melting) conditions. The combined SiO_2, FeO_{total} and Al_2O_3 contents of the Öræfajökull rhyolites indicate a relatively dry magma. The Al_2O_3 content of the melts is positively correlated with P_{H_2O}, increasing with increasing H_2O content. The low Al_2O_3 content (13.1 wt.%) of the rhyolitic tephra is below the dehydration melting field (Thy et al., 1990; Beard and Lofgren, 1991).

Compared to most rhyolites and basalts in a mid-ocean ridge setting, Icelandic rhyolites and basalts generally have elevated K_2O content. This is even more pronounced in the flank zone rhyolites (Thy et al., 1990). The high K_2O content of 3.3 wt.% in the 1362 AD tephra is a typical example of the latter type. Experimental data show that the K_2O content of silicic melt formed by dehydration melting of a metabasaltic source is a function of the K_2O content of the starting material. Water-saturated melting, stabilizing residual amphibole, yields K_2O-poor melts (e.g. Beard and Lofgren, 1989; Thy et al., 1990; Beard and Lofgren, 1991). The high K_2O content of the Öræfajökull 1362 AD silicic tephra is consistent with a large proportion of fractional crystallization of a relatively dry melt as opposed to melting of a water-rich metabasaltic source containing residual amphibole. The Cl, Ba and Zr contents are higher in the Öræfajökull 1362 AD tephra (Table 1) than in average Icelandic rift-zone rhyolites, although some rift-zone rhyolites are within the same compositional range (Jonasson, 1994).

Igneous hornblende is stable in silicic melts at H_2O contents above 4–5 wt.%, and temperatures less than about 950 °C at all crustal pressures (Burnham, 1979; Naney, 1983; Merzbacher and Eggler, 1984; Rutherford and Devine, 1988). Such H_2O contents require a minimum total pressure of 0.1 GPa, with $P_{total} \geq P_{H_2O}$ (Burnham, 1979). The lack of amphibole in the Öræfajökull silicic rocks, as well as in most other Icelandic rhyolites (e.g. Grönvold, 1972; Jonasson, 1994), indicates that the H_2O contents of the melts prior to eruption were less than 3–4 wt.%. The main exception to the general lack of amphibole in Icelandic rhyolites is found in the Torfajökull central volcano, which is the largest silicic centre in Iceland (e.g. Gunnarsson et al., 1998). The Torfajökull volcanic system is also the largest and most powerful high-temperature geothermal area in Iceland, with extensive and pervasive hydrothermal alteration. The appearance of amphibole in the silicic melts may therefore be related to supply of hydrothermal solutions to the melt either directly from groundwater or via anatectic contributions from hydrothermally altered wall rocks.

8.2. Rhyolite petrogenesis in volcanic rift zones and flank zones

The Icelandic rift zones are continuously covered by new lava flows and hyaloclastite deposits, while older units subside under the surface load. The volcanic productivity of the Icelandic rift zones is anomalously high relative to the half-spreading rate of 10 km/Ma, resulting in rapid subsidence of the partially altered and hydrated volcanic pile. Pálmason (1973) and Oskarsson

et al. (1982) developed models for crustal accretion and petrogenesis in Iceland.

Major and trace element compositional variation and a strong decrease in $^{18}O/^{16}O$ ratios from basalts to rhyolites indicate that anatexis of the hydrothermally altered pile of subsiding basalts contributes significantly to the generation of silicic melts in the rift-zone central volcanoes (e.g. O'Nions and Grönvold, 1973; Sigvaldason, 1974; Muehlenbachs et al., 1974; Oskarsson et al., 1982; Hemond et al., 1988; Nicholson et al., 1991; Jonasson, 1994; Gunnarsson et al., 1998). Melting of magma chamber wall rocks is promoted by fractional crystallization of the mafic to intermediate magmas. The presence of live ^{10}Be ($2.1–2.9 * 10^6$ atoms/g) in fresh obsidian samples from central volcanoes of the Icelandic rift zones demonstrates further that the time period from hydrothermal alteration to crustal melting is short and that ^{10}Be is partitioned efficiently from the hydrothermal fluid via the alteration assemblage to the partial melt (Grönvold et al., 2000).

The existing geochemical data for a range of basaltic, intermediate and silicic rocks of the Öræfajökull system demonstrates a different scenario (Prestvik et al., 2001). The O–Sr–Nd–Pb isotopic data show no systematic and significant difference between the basaltic, intermediate and rhyolitic units. O-isotopic data for other flank zone volcanic systems, e.g. the Snæfell, Vestmannaeyjar, Snæfellsjökull and Ljósufjöll, demonstrate a similar uniformity between evolved rocks and basalts (Sigmarsson et al., 1992; Hards et al., 2000). The analogous phase relations of the 1362 AD tephra and the Bushveld and Skaergaard granophyres may support the contention that the production of intermediate and silicic melts in Öræfajökull is mostly a result of fractional crystallization.

The indication that the volcanic flank zone magmas formed and evolved under lower water activity than the rift zone magmas is consistent with the lack of extensive geothermal activity in the flank zone central volcanoes. This limits the hydration of the crust and may lead to more extensive fractional crystallization accompanied by latent heat dissipation without bringing the wall rocks to their solidus temperatures. The limited amounts of crustal anatexis in the silicic melt generation may be understood in light of the thicker, cooler and stronger non-rifting crust and lithosphere. The more limited volcanic loading combined with cooler and stronger crust prevents significant subsidence of hydrated basalts.

8.3. Magma chamber volume and residence time

An erupted volume of 2 km^3 DRE rhyolitic tephra indicates a large magma reservoir prior to eruption. A rhyolitic melt fraction formed by fractional crystallization from basaltic via intermediate melt compositions constitutes 15–30% of the parental basaltic magma batch. The alternative model where rhyolitic melt is formed by crustal anatexis above and peripheral to a fractionating mafic magma reservoir would require similar volume relations (e.g. Oskarsson et al., 1982; Jonasson, 1994; Gunnarsson et al., 1998). The extraction of magma from crustal reservoirs is generally far from complete, with a commonly quoted extraction efficiency of 0.1–10% (e.g. Bower and Woods, 1998 and reference therein). Assuming that a magma chamber can erupt maximum 10% of its total volume, the Öræfajökull 1362 chamber was at least 20 km^3. A basaltic intrusion into such a large magma chamber would not necessarily result in eruption of basaltic lava fragments, but might result in a volume change and a heat flow perturbation in the magma chamber capable of triggering an eruption.

Shallow crustal magma chambers are geophysically indicated beneath the Icelandic volcanoes Krafla, Askja, Grimsvötn and Katla and are all in the rift zone (e.g. Gudmundsson et al., 1994; Brandsdottir et al., 1997; Gudmundsson and Milsom, 1997; Sturkell and Sigmundsson, 2000). The largest of these seems to be the Krafla chamber with an estimated volume of 12–54 km^3 (Brandsdottir et al., 1997).

Whereas petrogenetic and crustal deformation models of volcanoes often favour large magma chambers, some seismic attenuation studies have failed to detect such reservoirs. Under the active and frequently erupting Hekla volcano (6 eruptions since 1947), for instance, there is no seismic indication of any significant magma volume above 14 km depth (Soosalu and Einarsson, 2004). This is puzzling in view of the apparent need for a crystal fractionation chamber and the results from crustal deformation modeling, indicating a magma source located at 5–9 km depth (e.g. Kjartansson and Grönvold, 1983; Sigmundsson et al., 1992; Linde et al., 1993; Trygvason, 1994).

Seismic attenuation zones are also absent beneath the neighboring Torfajökull central volcano, which has erupted 3 times during the past 2000 years. The current seismicity pattern within the 12–18 km wide Torfajökull caldera indicate a cooling, but mostly solidified, magma body 4 km in diameter located at about 8 km depth (Soosalu and Einarsson, 2004). Therefore, magma chambers may be relatively short-lived features. This inference is supported by magma chamber fractionation times of about 10 years calculated from U-series disequilibria in samples from the Vestmannaeyjar volcanic systems (Sigmarsson, 1996). In general, recent U–Th-disequilibria studies of zero-age volcanic rocks indicate

that melt generation, porous flow, segregation, fractionation and eruption are surprisingly efficient and rapid processes (e.g. Turner et al., 1986; McKenzie, 2000).

There is no geophysical indication of any major upper crustal (<10–15 km depth) magma reservoir beneath Öræfajökull today, even if such reservoirs were present prior to the 1362 and 1727 eruptions. A time span of 300 years or less may well be sufficient for the generation and shallow injection (and/or eruption) of rhyolitic melt beneath Öræfajökull. The volcanic risk assessment for south Iceland should take such a scenario into account. A plinian eruption, equivalent to the 1362 event, would potentially have severe consequences for Iceland, especially during periods of prevailing easterly winds.

9. Conclusions

The investigated 1.8 m thick pyroclastic section from the Öræfajökull eruption of 1362 represents a tephra-fall deposit from a plinian or phreatoplinian eruption. The total erupted magma volume is estimated to 2 km^3 DRE and the plinian phase lasted probably 1–2 days. The high proportion of ash with grain size less than 250 μm (mostly 60–80 wt.%) and the predominance of thin-walled glass shards demonstrate a high degree of fragmentation driven by extensive gas release in the conduit. The grain-size variation through the investigated section indicates that the eruption had 3 intensity peaks of fragmentation.

The initial vent-clearing phase of the eruption is documented by large proportions of lithic fragments in the lowermost section (10–35 wt.% lithic fragments in the lowermost 10–15 cm of the section). The low amount of lithics in the rest of the section (<3 wt.%) indicates that the eruption continued from a single and stable vent. The vent location was probably within the 3–4 km wide summit caldera, which is covered by a glacier.

Remarkably homogenous melt and phenocryst compositions throughout the entire tephra section reflect a magma chamber where about 99 wt.% rhyolitic melt attained complete equilibrium with about 1 wt.% of oligoclase, hedenbergite and fayalite. The large eruption volume and the complete lack of other erupted magma compositions place important constraints on the total volume of the magma reservoir. Assuming a maximum fraction of erupted material of 10%, the total volume of the magma reservoir was at least 20 km^3. For a compositionally zoned magma chamber, with the homogeneous rhyolite confined to the uppermost part, this must be a very conservative estimate.

The currently largest shallow magma reservoir in Iceland inferred from geophysical data is the basaltic Krafla magma chamber (12–54 km^3), but the reservoir associated with the 1783 AD Laki eruption of 15 km^3 evolved basalt (Sigmarsson et al., 1991; Thordarson and Self, 1993) might have been 1–2 orders of magnitude larger.

The short timescales of magma generation, differentiation and magma chamber residence derived from U–Th-series disequilibrium studies (10–100 years) imply that the generation and evolution of a rhyolitic magma volume equivalent to the Öræfajökull 1362 reservoir can be accomplished within a few hundred years. This has important implications for the volcanic risk assessments of potentially very hazardous Icelandic rhyolite volcanoes like Öræfajökull.

Acknowledgements

Niels Óskarsson and Karl Grönvold suggested this investigation and provided logistical and scientific help during the field sampling and mineral analyses. Ármann Höskuldsson provided additional field assistance; Anette Mortensen and Jórunn Hardardóttir helped with the grain-size analyses; and Hiltrud Müller-Sigmund helped with the EMP analysis of the glasses. Niels Óskarsson, Hannes Mattsson, Heidi Soosalu and Anette K. Mortensen are thanked for valuable discussions, and Tore Prestvik reviewed an earlier version. Paul Hoskins corrected the English and anonymous referees reviewed the manuscript.

References

Beard, J.S., Lofgren, G.E., 1989. Effect of water on the composition of partial melting of greenstone and amphibolite. Science 244, 195–197.

Beard, J.S., Lofgren, G.E., 1991. Dehydration melting and water-saturated melting of basaltic and andesitic greenstone and amphibolites at 1, 3, and 6.9 kb. Journal of Petrology 32, 365–401.

Bower, S.M., Woods, A.W., 1998. On the influence of magma chambers in controlling the evolution of explosive volcanic eruptions. Journal of Volcanology and Geothermal Research 86, 67–78.

Brandsdottir, B., Menke, W., Einarsson, P., White, R.S., Staples, R.K., 1997. Faroe-Iceland Ridge experiment; 2, Crustal structure of the Krafla central volcano. Journal of Geophysical Research, B Solid Earth and Planets 102, 7867–7886.

Burnham, C.W., 1979. The importance of volatile constitutes. In: Yoder, H.S. (Ed.), The Evolution of the igneous rocks. 50th anniversary perspectives. Princeton University Press, pp. 439–482.

Grönvold, K., 1972. Structural and petrochemical studies in the Kerlingarfjöll region, Central Iceland. Ph.D. thesis, Oxford University.

Grönvold, K., Oskarsson, N., AlDahan, A.A.A., Possnert, G., 2000. ^{10}Be and the origin of Icelandic rhyolites. Eos Trans AGU 81, 1357 Suppl.

Gunnarsson, B., Marsh, B., Taylor, H.P., 1998. Generation of Icelandic rhyolites: Silicic lavas from the Torfajökull central Volcano. Journal of Volcanology and Geothermal Research 83, 1–45.

Gudmundsson, M.T., Milsom, J., 1997. Gravity and magnetic studies of the subglacial Grímsvötn volcano, Iceland: implications for

crustal and thermal structure. Journal of Geophysical Research 102, 7691–7704.
Gudmundsson, Ó., Brandsdóttir, B., Menke, W., Sigvaldason, G.E., 1994. The crustal magma chamber of the Katla volcano in south Iceland revealed by 2-D seismic undershooting. Geophysical Journal International 119, 277–296.
Hards, V.L., Kempton, P.D., Thompson, R.N., Greenwood, P.B., 2000. The magmatic evolution of the Snæfell volcanic centre; an example of volcanism during incipient rifting in Iceland. Journal of Volcanology and Geothermal Research 99, 97–121.
Helgason, J., Duncan, R.A., 2001. Glacial–interglacial history of the Skaftafell region, Southeast Iceland, 0–5 Ma. Geology 29, 179–182.
Hemond, C., Condomines, M., Fourcade, S., Al-legre, C.J., Oskarsson, N., Javoy, M., 1988. Thorium, strontium, and oxygen isotopic geochemistry in recent tholeiites from Iceland. Earth and Planetary Science Letters 87, 273–285.
Hildreth, W., 1981. Gradients in silicic magma chambers: implications for lithospheric magmatism. Journal of Geophysical Research 86 (B11), 10153–10192.
Johannesson, H., Saemundsson, K., 1998. Geological map of Iceland, 1:500,000, Bedrock Geology, 2nd edition. Icelandic Institute of Natural History, Reykjavik.
Jonasson, K., 1994. Rhyolite volcanism in the Krafla central volcano, north-east Iceland. Bulletin of Volcanology 56, 516–528.
Kaban, M.K., Flóvenz, O.G., Pálmason, G., 2002. Nature of the crust–mantle transition zone and the thermal state of the upper mantle beneath Iceland from gravity modelling. Geophysical Journal International 149, 281–299.
Kjartansson, E., Grönvold, K., 1983. Location of a magma reservoir beneath Hekla volcano, Iceland. Nature 301, 139–141.
Larsen, G., Dugmore, A.J., Newton, A.J., 1999. Geo0chemistry of historic-age silicic tephras in Iceland. Holocene 9, 463–471.
Larsen, G., Newton, A.J., Dugmore, A.J., Vilmundardottir, E.G., 2001. Geochemistry, dispersal, volumes and chronology of Holocene silicic tephra layers from the Katla volcanic system, Iceland. Journal of Quaternary Science 16, 119–132.
Linde, A.T., Augustsson, K., Sacks, I.S., Stefansson, R., 1993. Mechanism of the 1991 eruption of Hekla from continuous borehole strain monitoring. Nature 365, 737–740.
McKenzie, D., 2000. Constraints on melt generation and transport from U-series activity ratios. Chemical Geology 162, 81–94.
Merzbacher, C., Eggler, D.H., 1984. A magmatic geohydrometer: application to Mount St. Helens and other dacitic magmas. Geology 12, 587–590.
Muehlenbachs, K., Anderson, A.T., Sigvaldason, G.E., 1974. Low ^{18}O basalts from Iceland. Geochimica et Cosmochimica Acta 38, 577–588.
Naney, M.T., 1983. Phase equilibria of rock-forming ferromagnesian silicates in granitic systems. American Journal of Science 283, 993–1033.
Nicholson, H., Condomines, M., Fitton, J.G., Fallick, A.E., Grönvold, K., Rogers, G., 1991. Geochemical and Isotopic evidence for crustal assimilation beneath Krafla, Iceland. Journal of Petrology 32, 1005–1020.
Nielsen, T.F.D., 2004. The shape and volume of the Skaergaard intrusion, Greenland: implications for mass balance and bulk composition. Journal of Petrology 45, 507–530.
O'Nions, R.K., Grönvold, K., 1973. Petrogenic relationships of acid and basic rocks in Iceland and rare elements in late postglacial volcanics. Earth and Planetary Science Letters 19, 397–409.
Oskarsson, N., Sigvaldason, G.E., Steinthorsson, S., 1982. A dynamic model of rift zone petrogenesis and the regional petrology of Iceland. Journal of Petrology 23, 28–74.
Palais, J.M., Sigurdsson, H., 1989. Petrologic evidence of volatile emissions from major historic and pre-historic eruptions. In: Berger, et al. (Ed.), Understanding Climate Change. American Geophys. Union, Geophys. Monograph, vol. 52, pp. 31–53.
Palais, J.M., Taylor, K., Mayewski, P.A., Grootes, P., 1991. Volcanic ash from the 1362 A.D. Oraefajokull eruption (Iceland) in the Greenland ice sheet. Geophysical Research Letters 18, 1241–1244.
Pálmason, G., 1973. Kinematics and heat flow in a volcanic rift zone, with application to Iceland. Geophysical Journal of the Royal Astronomical Society 33, 451–481.
Pilcher, J., Bradley, R.S., Francus, P., Anderson, L., 2005. A Holocene tephra record from the Lofoten Islands, Arctic Norway. Boreas 34, 136–156.
Pilcher, J.R., Hall, V.A., McCormac, F.G., 1995. Dates of Holocene Icelandic volcanic eruptions from tephra layers in Irish peats. Holocene 5, 103–110.
Prestvik, T., 1979. Geology of the Öræfi district, southeastern Iceland. Nordic Volcanological Institute 7901. University of Iceland. 28 pp.
Prestvik, T., 1980. Petrology of hybrid intermediate and silicic rocks from Öræfajökull, southeast Iceland. Geologiska Föreningens i Stockholm Förhandlingar 101, 299–307.
Prestvik, T., 1985. Petrology of Quaternary volcanic rocks from Öræfi, southeast Iceland. Rep. 21Geological Institute, NTH. 81 pp.
Prestvik, T., Goldberg, S., Karlsson, H., Grönvold, K., 2001. Anomalous strontium and lead isotope signatures in the off-rift Öræfajökull central volcano in south-east Iceland. Evidence for enriched endmember(s) of the Iceland mantle plume? Earth and Planetary Science Letters 190, 211–220.
Rutherford, M.J., Devine, J.D., 1988. The May 18, 1980 eruption of Mount St. Helens: III. Stability and chemistry of amphibole in the magma chamber. Journal of Geophysical Research 93, 11949–11959.
Sigmarsson, O., 1996. Short magma chamber residence time at an Icelandic volcano inferred from U-series disequilibria. Nature 382, 440–442.
Sigmarsson, O., Grönvold, K., Condomines, M., Thotdarson, Th., 1991. Extreme magma homogeneity of the Lakagígar (Laki) eruption 1783–84, Iceland. Geophysical Research Letters 18 (12), 2229–2232.
Sigmarsson, O., Condomines, M., Forcade, S., 1992. Mantle and crustal contribution in the genesis of recent basalts from off-rift zones in Iceland: Constraints from Th, Sr and O isotopes. Earth and Planetary Science Letters 110, 149–162.
Sigmundsson, F., Einarsson, P., Bilham, R., 1992. Magma chamber deflation recorded by the Global Positioning System: the Hekla 1991 eruption. Geophysical Research Letters 19, 1483–1486.
Sigurdsson, H., 1982. Ubreidsla íslenskra gjóskulaga á botni Atlantshafs. Eldur er í Nordri. Sögufélag, Reykjavík, pp. 119–127.
Sigvaldason, G.E., 1974. The petrology of Hekla and origin of silicic rocks in Iceland. Eruption of Hekla 1974–1948 5,1, vol. 5. Societas Scientiarium Islandica, pp. 1–44.
Soosalu, H., Einarsson, P., 2004. Seismic constraints on magma chambers at Hekla and Torfajökull volcanoes, Iceland. Bulletin of Volcanology 66, 276–286.
Sturkell, E., Sigmundsson, F., 2000. Continuous deflation of the Askja caldera Iceland, during the 1983–1998 non-eruptive period. Journal of Geophysical Research, B Solid Earth and Planets 105, 25671–25684.
Thorarinsson, S., 1958. The Öræfajökull eruption of 1362. Acta Naturalia Islandica. II 2 99 pp.
Thorarinsson, S., 1967. Future Icelandic research concerning mid-ocean ridges and the upper mantle. Visindafelag Islendinga (Societae Scientiarum Islandica) 38, 201–207.
Thordarson, Th., Self, S., 1993. The Laki (Skaftár Fires) and Grimsvötn eruptions in 1783–1785. Bulletin Volcanologique 55, 233–263.

Thy, P., Beard, J.S., Lofgren, G.E., 1990. Experimental constraints on the origin of Icelandic rhyolites. Journal of Geology 98, 417–421.

Tryggvason, E., 1986. Multiple magma reservoirs in a rift zone volcano: ground deformation and magma transport during the September 1984 eruption of Krafla, Iceland. Journal of Volcanology and Geothermal Research 28, 1–44.

Trygvason, E., 1994. Observed ground deformation at Hekla, Iceland prior to and during the eruptions of 1970, 1980–1981 and 1991. Journal of Volcanology and Geothermal Research 61, 281–291.

Turner, S., Evans, P., Hawkesworth, C., 1986. Ultrafast source-to-surface movement of melt at island arcs from ^{226}Ra–^{230}Th systematics. Science 292, 1363–1366.

Wager, L.R., Brown, GM., 1968. Layered Igneous Rocks. Oliver and Boyd, Edinburgh.